Power line harmonic radiation observed by the DEMETER spacecraft at 50/60 Hz and low harmonics

Frantisek Nemec, Michel Parrot, O Santolík

AGU PUBLICATIONS

JGR

Journal of Geophysical Research: Space Physics

RESEARCH ARTICLE

10.1002/2015JA021682

Power line harmonic radiation observed by the DEMETER spacecraft at 50/60 Hz and low harmonics

F. Němec[1], M. Parrot[2], and O. Santolík[1,3]

[1]Faculty of Mathematics and Physics, Charles University in Prague, Prague, Czech Republic, [2]LPC2E/CNRS, Orléans, France, [3]Institute of Atmospheric Physics, The Czech Academy of Sciences, Prague, Czech Republic

Key Points:
- PLHR frequencies in excellent agreement with base power system frequencies
- Intensity increases at low odd harmonics are routinely detected, and low even harmonics are generally absent
- PLHR intensity increases at the times of higher GIC proxy values during the night

Correspondence to:
F. Němec,
frantisek.nemec@gmail.com

Citation:
Němec, F., M. Parrot, and O. Santolík (2015), Power line harmonic radiation observed by the DEMETER spacecraft at 50/60 Hz and low harmonics, *J. Geophys. Res. Space Physics*, *120*, 8954–8967, doi:10.1002/2015JA021682.

Received 13 JUL 2015
Accepted 22 SEP 2015
Accepted article online 27 SEP 2015
Published online 20 OCT 2015

Abstract We present a low-altitude satellite survey of Power Line Harmonic Radiation (PLHR), i.e., electromagnetic waves radiated by electric power systems on the ground. We focus on frequencies corresponding to the first few harmonics of the base power system frequencies (50 Hz or 60 Hz, depending on the region). It is shown that the intensities of electromagnetic waves detected at these frequencies at an altitude of about 700 km are significantly enhanced above industrialized areas. The frequencies at which the wave intensities are increased are in excellent agreement with base power system frequencies just below the satellite location. We also investigate a possible presence of the weekend effect, i.e., if the situation is different during the weekends when the power consumption is lower than during the weekdays. Such an effect might be possibly present in the European region, but it is very weak. PLHR effects are less often detected in the summer, as the ionospheric absorption increases, and also, the radiation is obscured by lightning generated emissions. This difference is smaller in the U.S. region, in agreement with the monthly variations of the power consumption. The analysis of the measured frequency spectra reveals that although intensity increases at low odd harmonics of base power system frequencies are routinely detected, low even harmonics are generally absent. Finally, we verify the relation of PLHR intensities to the geomagnetically induced currents (GICs) proxy. It is shown that the PLHR intensity is increased at the times of higher GIC proxy values during the night.

1. Introduction

Electric power systems on the ground radiate electromagnetic waves at harmonics of the base power system frequency. These waves penetrate to the upper ionosphere, where they can be detected by low-altitude satellites [*Tomizawa and Yoshino*, 1985; *Molchanov and Parrot*, 1995; *Rodger et al.*, 1995; *Němec et al.*, 2006, 2007, 2008]. Such electromagnetic wave events are typically called Power Line Harmonic Radiation (PLHR). When represented in a traditional form of frequency-time spectrograms with color-coded power spectral density of electric/magnetic field fluctuations, these events have a form of several narrow horizontal lines (i.e., they occur at constant frequencies). The frequency separation of these lines depends on the base power system frequency in the generation region, and it is equal either to 50/100 Hz or 60/120 Hz, because odd or even harmonics may be strongly suppressed in some cases [*Němec et al.*, 2006, 2007].

Although the intensity of the PLHR events is generally rather low, they may trigger new electromagnetic emissions [*Park and Helliwell*, 1983; *Nunn et al.*, 1999; *Parrot and Němec*, 2009; *Parrot et al.*, 2014] and possibly contribute to electron precipitation [*Tatnall et al.*, 1983; *Bullough*, 1995; *Prakash et al.*, 2009]. Propagation of PLHR events from their source power line up to the satellite altitudes was considered by *Kikuchi* [1983], *Ando et al.* [2002], *Němec et al.* [2008], and *Jing et al.* [2014]. Numerical results obtained by *Ando et al.* [2002] and *Jing et al.* [2014] show that while the effect of the radiation from a power line is limited to a relatively small geographical region at frequencies below the Earth-ionosphere waveguide cutoff frequency, the affected region becomes much larger if guided modes exist.

An interesting but disputable phenomenon is a possible existence of a week periodicity in the data related to the week cycle in the load of the electric power systems. *Park and Miller* [1979] suggested this as a possible explanation of why the overall wave intensity in the 2 to 4 kHz range detected on the ground at Siple, Antarctica, showed a distinct minimum on Sunday in comparison with the rest of the week. A similar dependence was obtained by *Parrot* [1991] using low-altitude Aureol-3 satellite data and a frequency filter centered around 72 Hz. The electric field component parallel to the Earth's magnetic field had a modulation depending

on days of the week. The average detected amplitude was maximum on Monday, and it monotonically decreased until Saturday. *Molchanov et al.* [1991] suggested that this week variation may be not only due to a lower power consumption during weekends as compared to weekdays but also due to a different current distribution in power systems. However, no evidence of this effect was found in ground-based measurements made at Halley, Antarctica [*Rodger et al.*, 2000]. *Karinen et al.* [2002] showed that there is no statistically significant "weekend effect" in the global geomagnetic activity expressed by the A_p index. They suggested that the previously reported presence of the weekend effect [*Fraser-Smith*, 1979] might be only a statistical fluctuation. Finally, *Němec et al.* [2010] analyzed 148 PLHR events identified in the DEMETER spacecraft data, and they reported that the events do not seem to occur less/more often during weekends than during weekdays.

Němec et al. [2006, 2007, 2008, 2010] used high-resolution wave data measured by the low-altitude DEMETER spacecraft along with an automatic identification of PLHR events to perform their systematic analysis. Their automatic identification procedure of PLHR events was, however, limited only to frequencies between 500 and 4000 Hz, as this was the frequency interval where formerly reported PLHR events occurred. In the present paper we focus on the analysis of ELF waves at frequencies corresponding to the first few harmonics of the base power system frequency. The data set is described in section 2. The obtained results are presented in section 3, and they are discussed in section 4. Finally, section 5 presents a brief summary of main results.

2. Data Set

DEMETER was a low-altitude spacecraft which operated between 2004 and 2010. It had a nearly circular polar orbit with an altitude of about 700 km. The orbit was quasi Sun-synchronous; i.e., the spacecraft was always located either in the local day (about 10:30 LT) or in the local night (about 22:30 LT). The DEMETER spacecraft was equipped, among others, with electric and magnetic field instruments [*Berthelier et al.*, 2006; *Parrot et al.*, 2006]. However, as the magnetic field data contain a significant amount of spacecraft interferences, exclusively the electric field data will be used in the present study. Low-resolution data which are not sufficient for the intended analysis of PLHR are collected nearly continuously in the Survey mode. However, the required high-resolution data are available only above locations of a special interest, during the so-called Burst mode intervals. These data consist of a waveform of one electric field component with the sampling frequency of 40 kHz. The Fast Fourier Transform analysis is performed, and the frequency spectra with the frequency resolution of 1 Hz and the time resolution of 8 s are calculated. We process all available DEMETER VLF Burst mode measurements, and in total more than 1,500,000 frequency spectra are calculated. These frequency spectra are used in all the further analysis.

In addition to the electric field data measured by the DEMETER satellite, we used the magnetic field data measured by flux-gate magnetometers on the ground. The data come from the SuperMAG network [*Gjerloev*, 2012], and they contain data from 447 magnetometer stations all over the world sampled with 1 min time resolution. These data are used to calculate the geomagnetically induced current (GIC) proxy, following the procedure used by *Forbes and St. Cyr* [2008, 2010]. The GIC proxy at a given time is calculated from the magnetometer which is the closest to the spacecraft location at this time. One hour long time interval centered at the time of interest is considered, and the value of the time derivative of the magnetic field magnitude, dB/dt, is calculated every minute. The GIC proxy is then equal to the maximum of dB/dt values over the one hour long time interval. Note that only the horizontal component of the magnetic field is considered, as only the horizontal component induces GICs.

3. Results

Before proceeding with the systematic analysis of PLHR, it is instructive to show an example of a PLHR event in the form of a frequency-time spectrogram. The data were measured on 3 November 2009 after 10:01:32 UT. Figure 1a shows a map in geographic coordinates showing the satellite orbit above Europe where an example 50 Hz PLHR event was observed. The satellite orbit is shown by the black curve. The red full circles, which nearly merge in a continuous red line, correspond to the central times of individual frequency spectra. They were calculated for the entire interval with the Burst mode coverage. The resulting frequency-time spectrogram of power spectral density of electric field fluctuations is shown in Figure 1b. Note that the event was observed during the daytime half-orbit when the spacecraft moved from north to south. The thin intense horizontal line at 50 Hz corresponds to the PLHR event. The additional noisy structure at about 140 Hz and

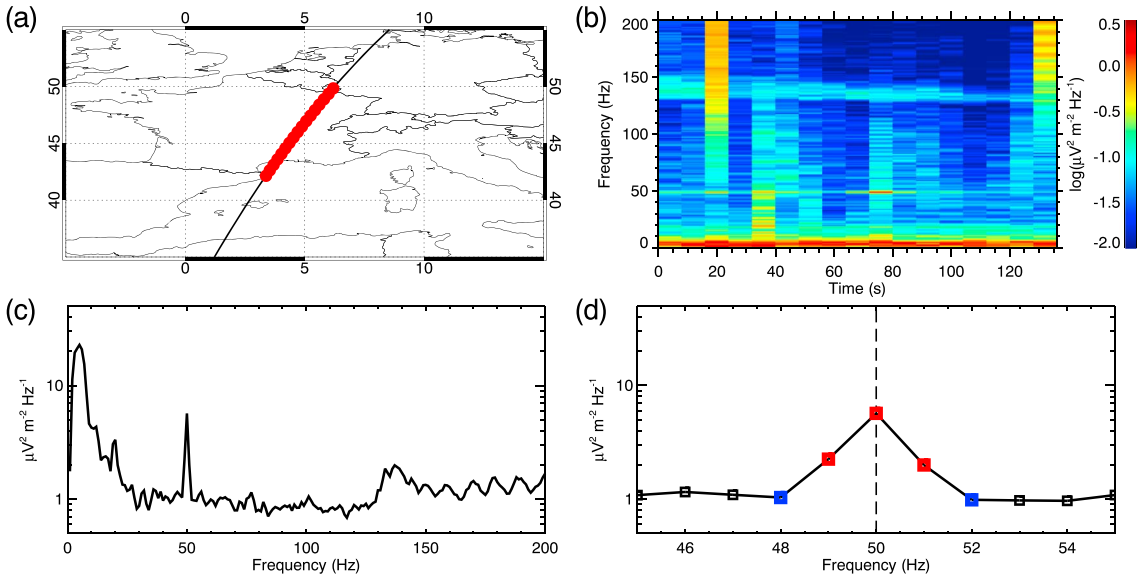

Figure 1. (a) Map in geographic coordinates showing the satellite orbit above Europe where an example 50 Hz PLHR event was observed. The satellite orbit is shown by the black curve, and the red full circles correspond to the central times of individual frequency spectra calculated during the Burst mode coverage. (b) Frequency-time spectrogram of power spectral density of electric field fluctuations calculated using the Burst mode data at the spacecraft locations marked in Figure 1a. The event was observed during the daytime half-orbit when the spacecraft moved from north to south. The thin intense horizontal line at 50 Hz can be clearly identified. (c) Frequency spectrum of the event. Note the sharp peak at 50 Hz corresponding to the PLHR event. (d) Zoomed frequency spectrum of the event demonstrating how the intensity of the PLHR event is determined, i.e., as a difference between the intensities of the red and blue points (see text). The data were measured on 3 November 2009 after 10:01:32 UT.

the short duration (i.e., vertical in the plot) broadband signals are formed by natural emissions, and they are not of interest for the present paper. The frequency spectrum corresponding to the frequency-time spectrogram from Figure 1b is shown in Figure 1c. The sharp peak at 50 Hz corresponding to the PLHR event can be clearly seen. A zoom of the frequency spectrum around this peak is shown in Figure 1d. The red points mark the frequencies 49 Hz, 50 Hz, and 51 Hz, i.e., the frequencies just around the PLHR central frequency. The blue points mark the frequencies 48 Hz and 52 Hz, i.e., the frequencies just slightly lower/larger than the frequencies of the PLHR event. We use the intensity difference between the red and the blue points to estimate the intensity $I_{50\mathrm{Hz}}^{\mathrm{PLHR}}$ of the PLHR as:

$$I_{50\mathrm{Hz}}^{\mathrm{PLHR}} = I_{49\mathrm{Hz}} + I_{50\mathrm{Hz}} + I_{51\mathrm{Hz}} - 1.5(I_{48\mathrm{Hz}} + I_{52\mathrm{Hz}}) \quad (1)$$

where I_f is the power spectral density of electric field fluctuations at the frequency f. Note that this calculation is done for each frequency spectrum separately. However, for the purpose of the example plot in Figure 1, we demonstrate the approach using the frequency spectrum of the entire event.

Figure 2 uses the same format as Figure 1 to show another example event, this time with a frequency of 60 Hz. The data were measured on 19 April 2009 after 15:21:02 UT. The event was observed above the northeastern part of the United States, and it again occurred during the daytime half-orbit when the spacecraft moved from north to the south. Curiously, the event is not limited exclusively to the base power system frequency (60 Hz), but it occurs also at the third harmonic (180 Hz). No increase of the wave intensity at 120 Hz, which would correspond to the second harmonic, is observed. We use the approach analogical to equation (1) to estimate intensities of 60 Hz events.

We use this approach for estimating the PLHR intensity of all frequency spectra measured by DEMETER in the Burst mode. Both possibilities, i.e., PLHR at a frequency of 50 Hz and PLHR at a frequency of 60 Hz, are investigated. The results obtained for PLHR frequencies of 50 Hz and 60 Hz are color coded as a function of geographic coordinates in Figures 3 and 4, respectively. The spatial bins of 5° × 5° are used, and occurrence rates p of I^{PLHR} larger than zero are color coded according to the scales at the top. The occurrence rate p in a given spatial bin is defined as

$$p = \frac{N(I^{\mathrm{PLHR}} > 0)}{N_{\mathrm{tot}}} \quad (2)$$

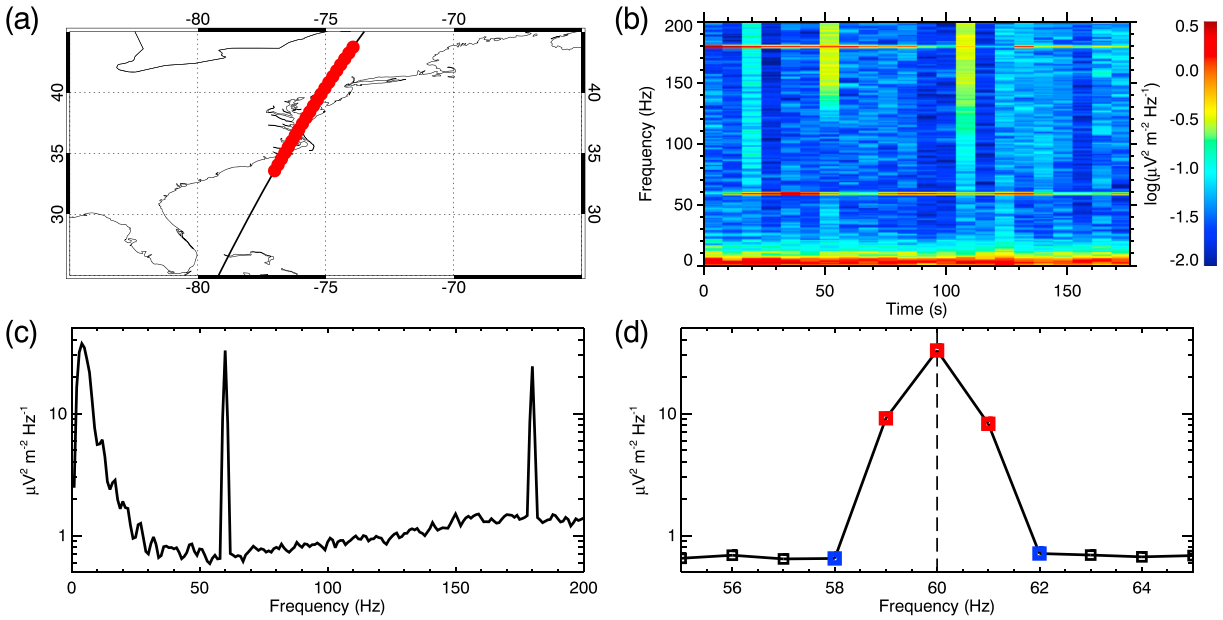

Figure 2. The same as Figure 1, but for an example 60 Hz event observed above the northeast United States. The event was again observed during the daytime half-orbit when the spacecraft moved from north to south. The PLHR event is seen at frequencies of 60 Hz and 180 Hz. The data were measured on 19 April 2009 after 15:21:02 UT.

where $N(I^{PLHR} > 0)$ is the number of frequency spectra with $I^{PLHR} > 0$ and N_{tot} is the total number of frequency spectra in the bin. Only the values of p in spatial bins with $N_{tot} \geq 100$ are plotted. If there was no particular variation of the frequency spectrum at frequencies of 50/60 Hz, the resulting occurrence rates p should be close to 0.5, corresponding to the situation of an equally probable increase and decrease of the wave intensity. On the other hand, if there was an increase of the wave intensity at 50/60 Hz, p should be larger than 0.5.

The geographic map of the occurrence rate p at the frequency of 50 Hz shown in Figure 3 reveals that while the occurrence rates are close to 0.5 at the longitudes of America, there is a large area of above average occurrence

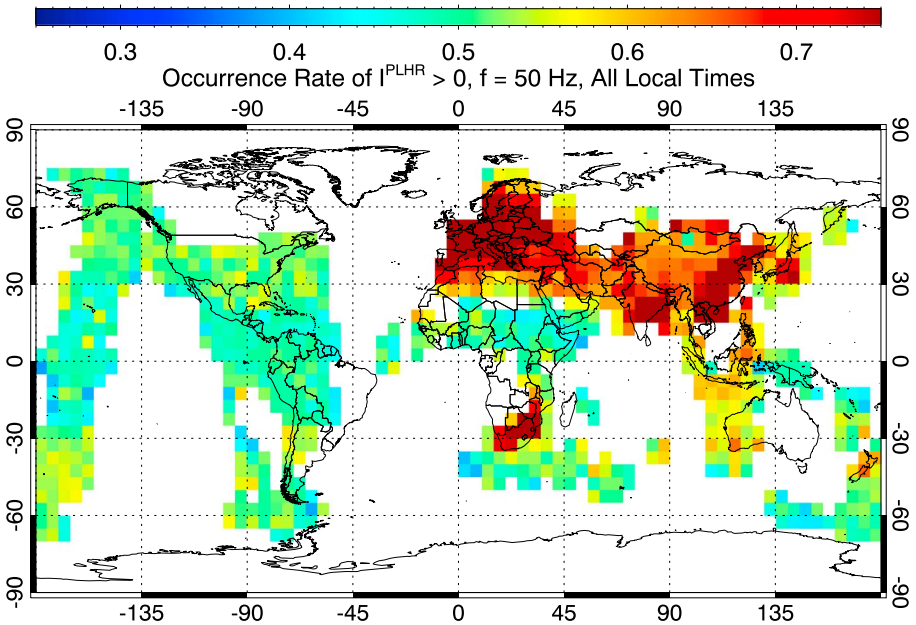

Figure 3. Geographic map showing the occurrence rate of increased wave intensity at 50 Hz (see text). The color scale at the top is used. The spatial resolution of individual bins is 5° × 5°. The large area of above average occurrence rates can be seen above Europe and Asia. An additional area of above average occurrence rates is in South Africa.

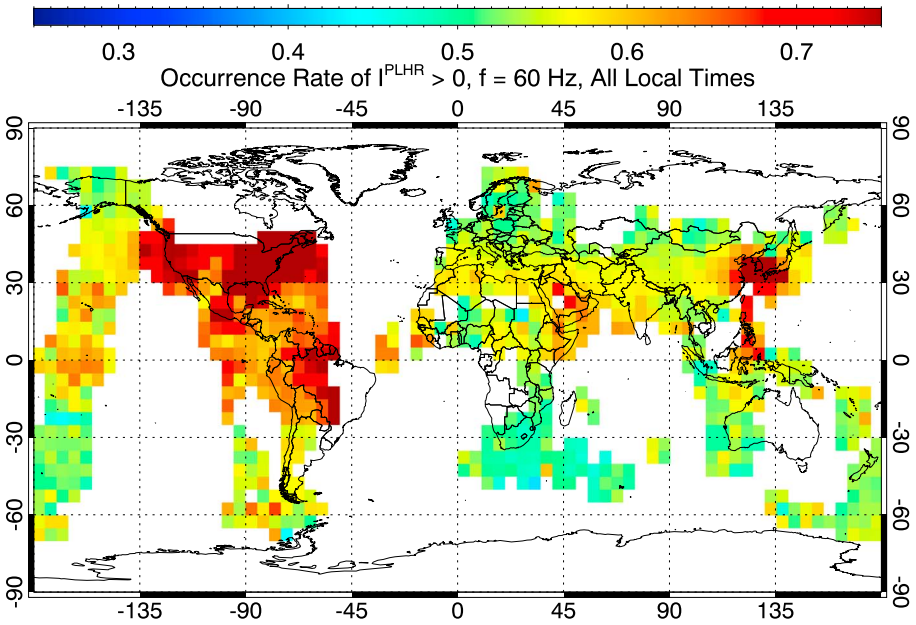

Figure 4. The same as Figure 3 but for the wave intensity at 60 Hz. The large area of above average occurrence rates can be seen above America. Additional areas of above average occurrence rates are around Japan and Arabia.

rates p above Europe and Asia. An additional area of above average occurrence rates can be identified in South Africa. The geographic map obtained for the frequency of 60 Hz and depicted in Figure 4 shows a rather different situation. The occurrence rates p are enhanced predominantly above North America (particularly both East and West Coasts) and Japan. An additional area of above average occurrence rates can be identified above Arabia.

One can see that the areas where the occurrence rates p at 50 Hz and 60 Hz are larger than elsewhere correspond well to the industrialized regions with their respective base power system frequencies. This is further confirmed by a comparison with Figure 5, which shows the world map of power consumption and the base power system frequency. The average power consumption per square kilometer for individual countries is color coded using different tones according to the color scales on the top. It was calculated as the average annual electric power consumption in 2004–2010 (http://data.worldbank.org/indicator/EG.USE.ELEC.KH) divided by the country area. Moreover, the base power system frequency in individual countries is distinguished. Specifically, the blueish color scale is used for countries which have the base power system frequency of 50 Hz, and the reddish color scale is used for countries which have the base power system frequency of 60 Hz. We note that Japan is split in two parts in this color coding, as its western part uses 60 Hz, while its eastern part uses 50 Hz. Nevertheless, the average power consumption is calculated for the entire Japan, in the same way as for all other countries. The fact that a single value of the average power consumption is calculated for each country necessarily results in significant local inaccuracies at regions of large countries whose power consumption is substantially different from the country average. However, one can see excellent overall agreement between the areas of enhanced occurrence rates p at 50/60 Hz and the countries with high average power consumption using a given base power system frequency.

Having shown that the intensity of electromagnetic waves detected by the DEMETER spacecraft at frequencies of 50/60 Hz is on average enhanced above industrialized areas with respective base power system frequencies, it is interesting to verify whether a weekend effect is present in the data, i.e., whether the intensity increase is lower during weekends than during weekdays. This effect is investigated in Figure 6. We use the data measured during both the daytime and nighttime, and we focus on two highly industrialized regions which are well identifiable in overall maps in Figures 3 and 4: (i) "European region" (base power system frequency of 50 Hz, longitudes 0°–30°, latitudes 40°–60°), (ii) "U.S. region" (base power system frequency of 60 Hz, longitudes −100°–−70°, latitudes 30°–50°). Further analysis is limited only to these two regions.

Figure 6a shows the occurrence rate p at 50 Hz obtained for the European region as a function of the day of week. The thick horizontal line corresponds to the average occurrence rate $\bar{p}$ at 50 Hz in the European region.

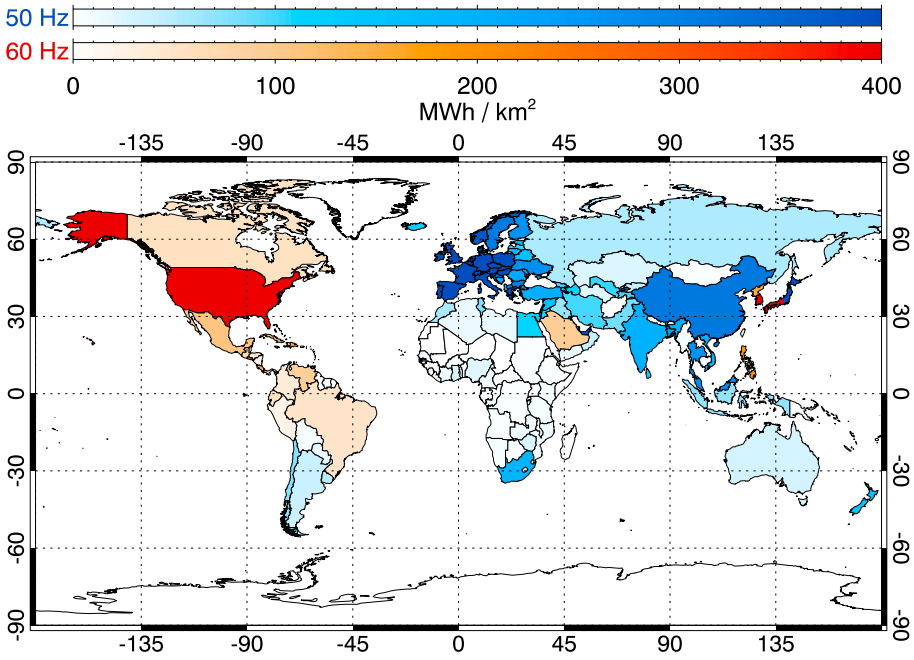

Figure 5. World map of power consumption and the base power system frequency. The average power consumption for individual countries is color coded according to the scales at the top (see text for more details on its calculation). The blueish color scale is used for countries which use the base power system frequency of 50 Hz, and the reddish color scale is used for countries which use the base power system frequency of 60 Hz.

The thin horizontal lines correspond to ±1 standard deviation from the mean value calculated as the standard deviation of a binomial distribution, i.e., $\sigma_p = \sqrt{(\bar{p}(1-\bar{p})/N}$, where N is the total number of frequency spectra measured at a given day of the week. The red and blue colors of individual vertical bars are used only to distinguish weekdays (red) from weekends (blue). Figure 6b uses the same format as Figure 6a, but it shows the results obtained for wave intensities at 60 Hz observed above the U.S. region. Moreover, the average hourly power consumption in the U.S. region (http://www.ferc.gov/docs-filing/forms/form-714/data.asp) is overplotted using the thick black line with diamonds and the scale on the right. These data are from the FERC (Federal Energy Regulatory Commission) form no. 714. This form collects the hourly load for each day of a given year from all U.S. electric systems. In this study the year 2008 has been considered, and the data of 147 electric generating plants have been added (excluding Alaska and Hawaii). The average daily consumption in 2008 was evaluated for individual days of week. U.S. national holidays were counted as Sundays. It is interesting to note that the largest electric power consumptions are in the following states: Texas, California, Florida, Ohio, New York, Illinois, and Pennsylvania. This is in agreement with the map shown in Figure 4.

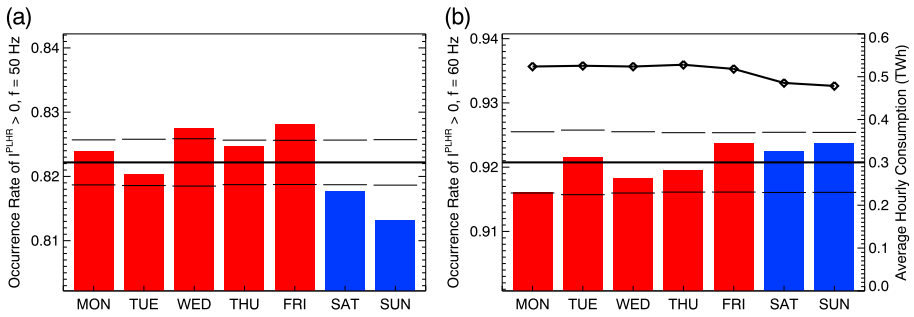

Figure 6. (a) Occurrence rate of increased wave intensities at 50 Hz obtained for the European region as a function of the day of week. The thick horizontal line corresponds to the average occurrence rate at 50 Hz in the European region. The thin horizontal lines correspond to ±1 standard deviation from the mean value. (b) The same as the Figure 6a) but for wave intensities at 60 Hz and the U.S. region. The average hourly power consumption is overplotted using the thick black line with diamonds and the scale on the right.

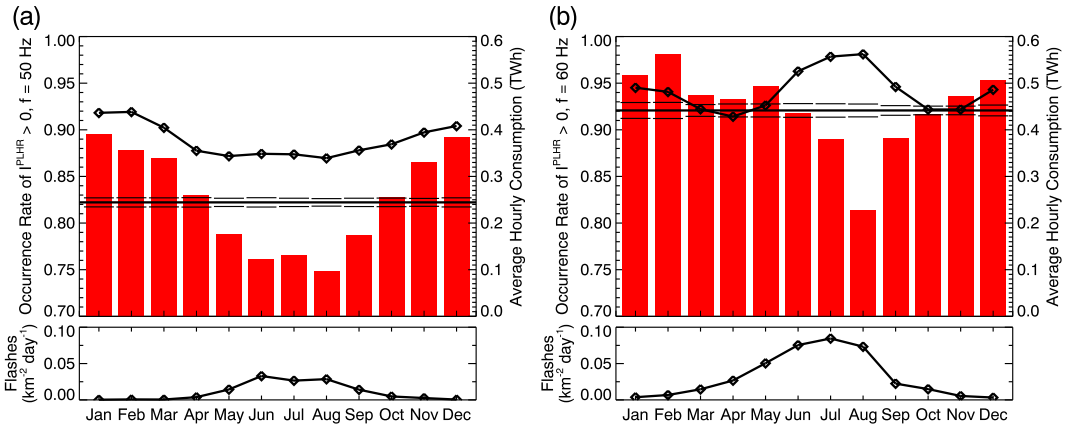

Figure 7. (top) Monthly variation of the occurrence rate of increased wave intensities, along with the monthly variation of the average hourly power consumption. The used format is the same as in Figure 6b. (bottom) Monthly variation of the average lightning activity. Figure 7a was obtained for the European region and 50 Hz, and Figure 7b was obtained for the U.S. region and 60 Hz.

As can be seen in Figure 6b, the average hourly power consumption in the U.S. region is lower during weekends than during weekdays by about 8%. However, the occurrence rates at 60 Hz do not follow this dependence, and they are nearly independent on day of the week. In fact, there seems to be a minor enhancement of the occurrence rate on Sunday, and a minor decrease of the occurrence rate on Monday, i.e., the trend just opposite to the one expected. On the other hand, the results shown in Figure 6a suggest that there might be a weekend effect present in the data measured in the European region. It is, however, very weak. Specifically, the occurrence rate p in the European region is by about 0.01 lower during weekends that during weekdays. We note that there are no overall data of average hourly power consumption available for Europe. We also emphasize that the situation is, in general, significantly more complicated, as the electric power consumption exhibits not only a week cycle, but also an annual cycle, which is related to different power requirements in the winter/summer seasons. One should also consider a daily variation and a limited local time sampling of the DEMETER spacecraft. This will be discussed more in detail in section 4.

Variations of the occurrence rate p due to the annual cycle of the power consumption are investigated in Figure 7. Figure 7a (top) shows a monthly variation of the occurrence rate at 50 Hz obtained for the European region. The used format is the same as in Figure 6b. The power consumption data corresponding to the year 2011 were obtained from the European Network Transmission System Operators for Electricity (https://www.entsoe.eu/publications/statistics/monthly-statistics). It can be seen that both the occurrence rate p and the average hourly power consumption have a well-pronounced minima in the summer. Specifically, the average hourly power consumption is by more than 15% and the occurrence rate p by more than 0.12 lower during the summer than during the winter. The situation in the U.S. region depicted in Figure 7b is rather different. The average power consumption data for years 2005–2010 were obtained from the U.S. Energy Information Administration (http://www.eia.gov/electricity/monthly). Due to an extensive use of the air condition, the power consumption has a maximum rather than a minimum in the summer. However, the monthly variation of the occurrence rate p at 60 Hz exhibits a decrease in the summer, particularly in August. Specifically, while the average hourly power consumption is by more than 20% larger during the summer than during spring/autumn, the occurrence rate p is on average by more than 5% lower (and by more than 10% lower in August).

The interpretation of these dependencies is complicated, as other factors than the average hourly power consumption also exhibit annual variations. In particular, the lightning activity has a maximum in the local summer. This is demonstrated by the average flash rate in the European and U.S. regions shown in Figure 7 (bottom rows). The average flash rate data were obtained from the High Resolution Monthly Climatology (HRMC) Lightning Imaging Sensor/Optical Transient Detector (LIS/OTD) gridded climatology data set [*Cecil et al.*, 2014]. It can be seen that the maxima in the lightning occurrence approximately correspond to the minima in the occurrence rate p. Taking into account that the lightning generated emissions contribute significantly to the overall wave intensity, this may be possibly understood in terms of PLHR emissions being too weak to be properly detected at the times of intense lightning generated background. One must also consider

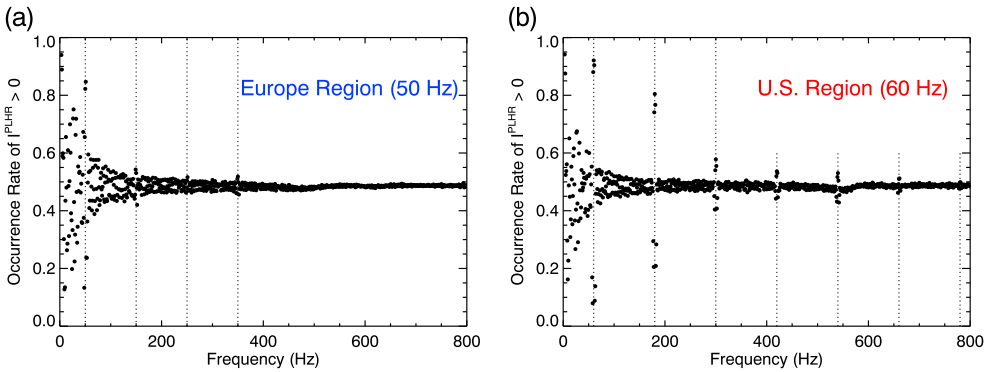

Figure 8. (a) Occurrence rate of increased wave intensities (see text) obtained for the European region as a function of the frequency. The dotted vertical lines at 50 Hz, 150 Hz, 250 Hz, and 350 Hz mark the harmonics of the base power system frequency where the occurrence rate is enhanced. (b) The same as the Figure 8a but for the U.S. region. The dotted vertical lines at 60 Hz, 180 Hz, 300 Hz, 420 Hz, 540 Hz, 660 Hz, and 780 Hz again mark the harmonics of the base power system frequency where the occurrence rate is enhanced.

that in the summer, the radiation coming from the Earth's surface is more attenuated during the propagation through the ionosphere because of larger electron densities. It is thus difficult to relate the observed monthly variation of the occurrence rate p directly to the monthly variation of the power consumption.

Figure 2, as well as former results concerning PLHR, demonstrate that PLHR is observable not only at base power system frequencies but also at the corresponding harmonics. We investigate this phenomenon for the European and U.S. regions in more detail in Figures 8a and 8b, respectively. Occurrence rates p obtained for the respective regions are plotted as a function of the frequency. Exactly the same procedure as the one used for calculating I^{PLHR} (equation (1)) was used, but it was extended to frequencies other than 50/60 Hz. The dotted vertical lines correspond to odd harmonics of the base power system frequency. Specifically, for the European region, these frequencies are 50 Hz, 150 Hz, 250 Hz, and 350 Hz. For the U.S. region these frequencies are 60 Hz, 180 Hz, 300 Hz, 420 Hz, 540 Hz, 660 Hz, and 780 Hz. We note that the occurrence rates p increase at odd harmonics of the base power system frequency and they decrease at frequencies just around them. This directly stems from the definition of I_{PLHR} (equation (1)). Specifically, I_{PLHR} at the frequencies close to the odd harmonics is obtained by subtracting the enhanced intensities at odd harmonics, i.e., it tends to get negative. It is also curious to note that PLHR extends to higher harmonic numbers in the U.S. region than in the European region. Finally, we note that the high fluctuations of the occurrence rates at low frequencies (<50 Hz) correspond to the high-intensity noise typically observed in electric field spectrograms at these frequencies (see Figures 1b, 1c, 2b, and 2c).

Figure 9 is similar to Figure 8 in the sense that it also deals with the analysis of the frequency spectra observed in the European and U.S. regions. However, this time the median frequency spectra are evaluated rather than calculating the occurrence rates p at individual frequencies. This approach is more straightforward, as the resulting quantities remain in physical units and they are easier to interpret. On the other hand, it is less sensitive to minor enhancements of the wave intensity at specific frequencies, as these might be easily obscured by the background noise (i.e., by electromagnetic waves detected by the DEMETER spacecraft which are not related to PLHR). Moreover, as the intensity of background depends on the local time, it is necessary to distinguish between the two local times sampled by DEMETER ("daytime" and "nighttime") and to plot the results for each of them separately. This was not needed in the aforementioned plots, as they contained the results with the background effectively subtracted. If the calculation is performed separately for the daytime and nighttime, the obtained results are similar (not shown), and only the results obtained without taking the local time into account were thus plotted.

Figure 9a shows the median daytime frequency spectrum obtained for the European region by the thick curve. The thin curves show the 0.25 and 0.75 quartiles. The dotted vertical lines at 50 Hz and 150 Hz mark the harmonics of the base power system frequency where the power spectrum is enhanced. Note that the broad peak at the frequency spectrum at about 140 Hz is due to natural emissions, and it is not related to PLHR. A signature of these emissions can be in fact identified already in Figure 1b. Figures 9b–9d use the same representation to show results obtained for other combinations of European/U.S. region and day/night. Namely,

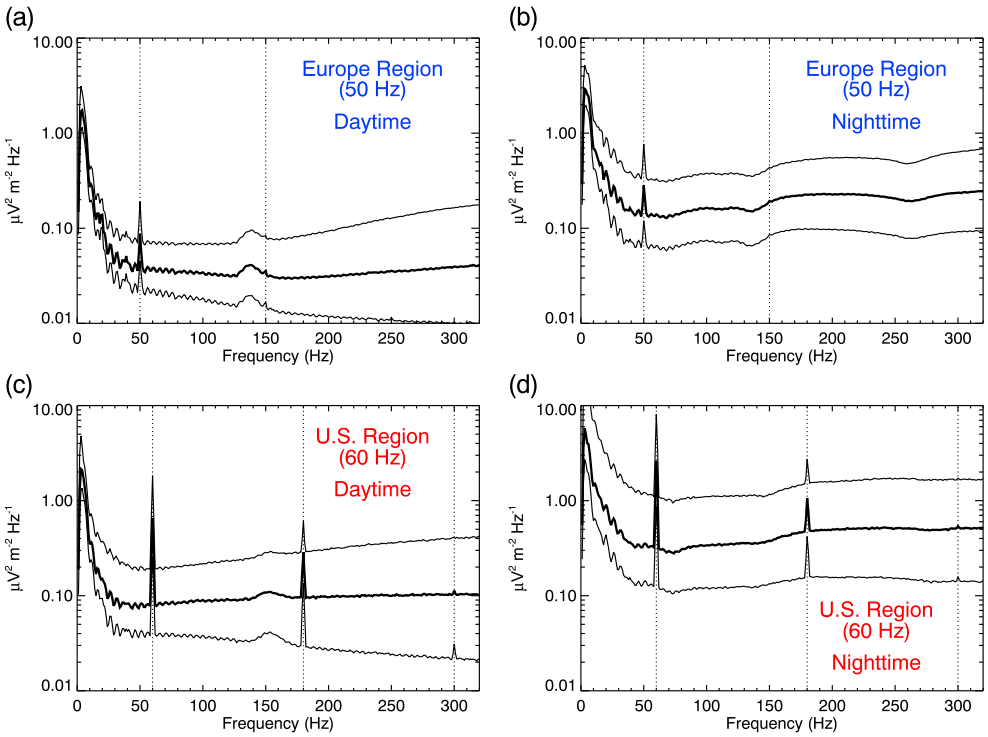

Figure 9. (a) Median daytime frequency spectrum obtained for the European region is shown by the thick curve. The thin curves show the 0.25 and 0.75 quartiles. The dotted vertical lines at 50 Hz and 150 Hz mark the harmonics of the base power system frequency where the power spectrum is enhanced. Note that the broad peak in the frequency spectrum at about 140 Hz is natural and not related to PLHR. (b) The same as Figure 9a but for the European region nighttime. (c) The same as Figure 9a but for the U.S. region daytime. The dotted vertical lines at 60 Hz, 180 Hz, and 300 Hz mark the harmonics of the base power system frequency where the power spectrum is enhanced. Note that the broad peak in the frequency spectrum at about 160 Hz is natural and not related to PLHR. (d) The same as Figure 9c but for the U.S. region nighttime.

Figure 9b was obtained for the European region nighttime, Figure 9c was obtained for the U.S. region daytime, and Figure 9d was obtained for the U.S. region nighttime. The wave intensities in the U.S. region are increased at 60 Hz, 180 Hz, and 300 Hz, corresponding again to odd harmonics of the 60 Hz base frequency. Note that the broad peak in the frequency spectrum at about 160 Hz in Figure 9c is due to natural emissions, and it is not related to PLHR. This peak is at higher frequencies in the U.S. region than in the European region due to the higher geomagnetic latitudes of the U.S. region.

The variations in PLHR intensity for different GIC levels are shown in Figure 10. Median daytime frequency spectrum obtained for the European region at the times of low GIC proxy values (<1 nT/min) is shown in Figure 10a by the blue curve. Median daytime frequency spectrum obtained for the European region at the times of high GIC proxy values (> 5 nT/min) is shown by the red curve. The dotted vertical line at 50 Hz marks the base power system frequency, where the intensity is enhanced. Figures 10b–10f use the same representation to show results obtained for other combinations of European/U.S. region and day/night. Namely, Figure 10b was obtained for the European region nighttime, Figure 10c was obtained for the U.S. region daytime, and Figure 10d was obtained for the U.S. region nighttime. Moreover, as a significant intensity increase in the U.S. region is observed not only at 60 Hz but also at 180 Hz, Figure 10e shows the results obtained for the U.S. region daytime at frequencies close to 180 Hz, and Figure 10f shows the results obtained for the U.S. region nighttime at frequencies close to 180 Hz.

One can see that the median intensity at the base power system frequencies/third harmonic in the U.S. region is increased both for low and large levels of GIC proxy, forming distinct peaks in the center of individual plots. The median intensities observed during large GIC proxy values (red curves) are systematically larger than the median intensities observed during low GIC proxy values (blue curves). This is true not only at the frequencies affected by PLHR but also all over the analyzed frequency range. The reason for this overall intensity

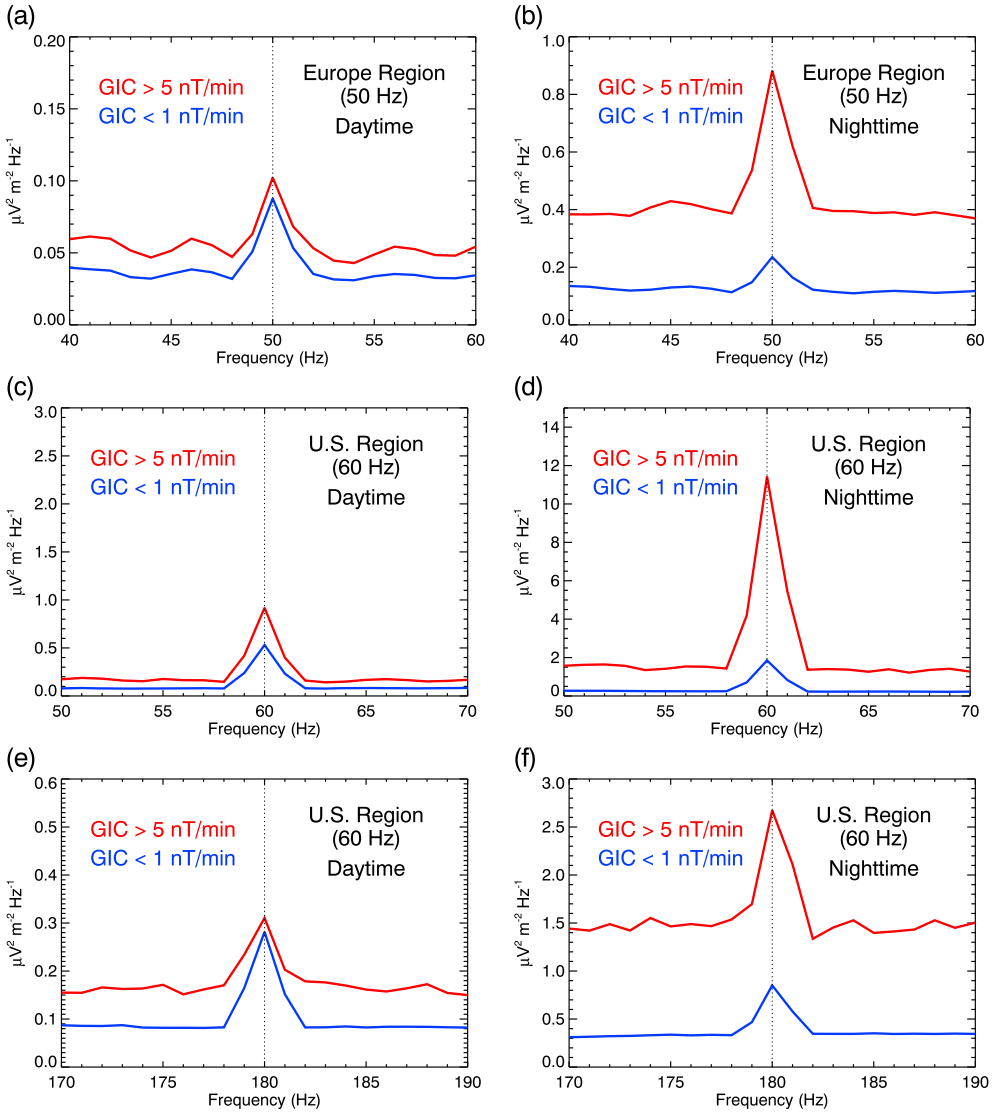

Figure 10. (a) Median daytime frequency spectrum obtained for the European region at the times of low GIC proxy values (<1 nT/min) is shown by the blue curve. Median daytime frequency spectrum obtained for the European region at the times of high GIC proxy values (> 5 nT/min) is shown by the red curve. The dotted vertical line at 50 Hz marks the base power system frequency, where the spectrum is enhanced. (b) The same as Figure 10a but for the European region nighttime. (c) The same as Figure 10a but for the U.S. region daytime. The dotted vertical line at 60 Hz marks the base power system frequency, where the spectrum is enhanced. (d) The same as Figure 10c but for the U.S. region nighttime. (e) The same as Figure 10c but for the peak at 180 Hz, i.e., the third harmonic of the base power system frequency. (f) The same as Figure 10e but for the U.S. region nighttime.

increase is that larger GICs generally correspond to geomagnetically disturbed periods, when the intensity of natural emissions increases significantly as compared to quiet times. In order to evaluate the dependence of PLHR on the GIC proxy, one should thus not compare the absolute values of the peaks at base power system frequency/harmonics but rather the difference between the peak intensity and the intensity at surrounding frequencies. As far as the daytime results are concerned, this intensity difference remains about the same in the European region. It somewhat increases at the times of large GIC proxy values in the U.S. region at 60 Hz, and it somewhat decreases at the times of large GIC proxy values in the U.S. region at 180 Hz. However, all these variations are rather weak. On the other hand, the nightside results show a rather different dependence. Namely, the PLHR intensities both in the European and U.S. regions are significantly increased at the times of large GIC proxy values. One should also note that during the night, both the overall intensities and their variation as a function of the GIC proxy values is considerably larger than during the day.

4. Discussion

The DEMETER spacecraft provided a large amount of high-resolution electromagnetic wave Burst mode data during the course of its more than 6 years of measurements. Although these were obtained primarily at locations of a special interest, i.e., their geographic distribution is far from being uniform, their overall coverage over the continents is reasonably good to allow a systematic analysis of PLHR in most industrialized areas. In contrast with former studies of PLHR, we do not focus on identification of individual PLHR events and their subsequent analysis but we directly analyze intensity variations at harmonics of the base power system frequency as a function of the geographic location. A huge advantage of this approach is that it does not rely on the identification procedure of PLHR events. Instead, it provides us with an overall average measure of the PLHR influence.

The base frequencies of the power system are assumed to be exactly equal to 50/60 Hz in the analysis. Although the real base frequency of a power system at a given time may be slightly different from these optimal values, its deviation should not typically exceed the 1 Hz frequency resolution used in the analysis. The deviation of the real power system frequency from the expected optimal value becomes more significant at higher harmonics. However, as the presented analysis is limited only to low harmonics of the base power system frequency, the frequency deviation will likely remain relatively small as compared to the used frequency resolution. We use this knowledge of PLHR frequencies to evaluate their intensity with respect to the intensity measured at neighboring frequencies. In order to account for not entirely sharp peaks in the frequency spectra, a 3 Hz frequency window is used to evaluate the PLHR intensity. The subtraction of the power spectral density at frequencies just around the PLHR frequency then allows us to evaluate how much the PLHR intensity stands out as compared to the surrounding background.

Having evaluated the PLHR intensity with respect to the surrounding background (i.e., whether there is an intensity decrease or an intensity increase at a given frequency), we calculate the occurrence rates p of an intensity increase as a function of relevant controlling parameters (geographic location, day of week, frequency). Although this approach is very simple, it turns out to be rather effective in dealing with the varying intensity of the natural background. Specifically, although the wave intensity measured by the DEMETER spacecraft is significantly different during the day and during the night, the applied data processing leads to comparable results during the day and during the night. This indicates that it is really the intensity increase due to PLHR which we evaluate, quite independently on the intensity of surrounding natural emissions.

The obtained geographic maps of occurrence rates at 50/60 Hz show remarkable agreement with the world map of power consumption and the base power system frequency. This demonstrates that above industrialized areas the wave intensity at frequencies corresponding to the base power system frequency is significantly enhanced above normal levels due to PLHR. It should be noted that the intensity increases are observed exclusively above the industrialized areas and not above their geomagnetically conjugate points, suggesting that the effects of PLHR are limited primarily to the hemisphere of origin.

There might be a weak signature of the weekend effect in the results obtained for the European region. No such signature, and even a sign of opposite behavior, is observed in the U.S. region (although power consumption data in the U.S. region exhibit a decrease during weekends). However, overall, the observed day-of-week variation in PLHR is extremely weak, if it is existent at all. This is likely at least partly related to the observational procedure. Namely, although specific, highly industrialized regions (European, U.S.) are selected for the analysis, all the observations are not performed above the same place and under the same conditions. The intensity of natural electromagnetic waves varies, and although our procedure attempts to filter out these variations, it is for sure an effect which tends to smooth out the (possible) day-of-week variation in PLHR. Another point is that neither the European nor the U.S. region can be considered as uniform, and that DEMETER samples them at random locations, which again results in smoothing out the (possible) day-of-week variation in PLHR. The week period is further smoothed out by the annual variations in the power consumption. One should also consider that the difference between the power consumption during weekends and weekdays is the largest during the day, when the efficiency of wave penetration through the ionosphere is rather low. On the other hand, during the nighttime, when the waves can more easily penetrate the ionosphere, the week periodicity is less pronounced. Finally, not only the overall power consumption but also the current distribution in power systems affects the intensity of PLHR [*Molchanov et al.*, 1991].

The magnitude of the annual variations in the power consumption is larger than the magnitude of the week variations. Unfortunately, the evaluation of their effects on the PLHR intensity is extremely difficult due to the annual cycle of other relevant factors. Among these, the lightning activity (peaking in the summer) seems to be particularly important. Lightning-generated electromagnetic waves contribute significantly to the overall wave intensity. An intense lightning activity can thus result in an intense electromagnetic background noise, which obscures PLHR. This might be a possible explanation of the occurrence rate p in the U.S. region having a minimum in the summer, although the power consumption is maximal. One should also possibly consider seasonal variations of other parameters, e.g., a seasonal variation of the wave attenuation during the propagation through the ionosphere (related to seasonal variations of ionospheric electron density profiles). A comparison of the situation in the European and in the U.S. regions reveals that the summer decrease in the occurrence rate p is significantly stronger in the European region than in the U.S. region, corresponding thus well to the respective changes in the power consumption.

The signatures of PLHR are observed not only at base power system frequencies, but also at their low harmonics. Generally, only odd harmonics are observed, while the intensity at even harmonics does not seem to be affected. This is consistent with ground-based measurements of power system harmonics [*Nunn et al.*, 1999; *Chen and Zhang*, 2012], and it can be likely understood in terms of positive and negative half-cycles of power system voltages and currents tending to have identical waveshapes, so that their Fourier series contain only odd harmonics [*Grady and Santoso*, 2001].

The median power spectral densities of PLHR in the European and U.S. regions range from tenths to units of $\mu V^2\ m^{-2}\ Hz^{-1}$ (see Figure 9). They are generally larger during the night than during the day, being consistent with the results obtained by *Němec et al.* [2008] for PLHR events detected at higher harmonics. This is likely related to the wave attenuation during the propagation through the ionosphere. The observed PLHR power is by about an order of magnitude larger than the intensity of PLHR events reported by *Němec et al.* [2008]. This is consistent with the expected lower radiated power at higher harmonics, as can be seen in Figures 9c and 9d. We also note that the PLHR intensity detected in the U.S. region is generally larger than the PLHR intensity detected in the European region, and moreover, more harmonics of the base power system frequency are observable in the U.S. region. Among differences in the overall power consumption, this might be possibly related to different distribution of power lines, with long high-voltage power lines occurring more often in the U.S. than in Europe.

PLHR intensities are significantly enhanced at the times of large GIC proxy values during the night. On the other hand, the change of PLHR intensities related to the variations of GIC proxy values is rather minor on the dayside. This might be consistent with the results obtained by *Viljanen et al.* [2001] and *Viljanen et al.* [2006], who showed that the diurnal occurrence of large GIC values exhibits a clear maximum around the magnetic midnight, which probably corresponds to the substorm activity. This is, however, not the case in the GIC proxy values we use, which are not significantly different during the night than during the day. A likely explanation for this discrepancy is the limited time resolution of the magnetometer data that we used for the calculation of GIC proxies (1 min), which is not able to capture all the short-term variability analyzed by *Viljanen et al.* [2001] and *Viljanen et al.* [2006], who used the data with time resolution of 1 s. Enhanced PLHR intensities at the times of large GICs are consistent with the case-study results reported by *Hayashi et al.* [1978]. A likely interpretation is that the quasi-DC current induced in a power line system distorts the power line current waveforms due to a transformer-core saturation, resulting thus in a more intense radiation [*Hayashi et al.*, 1978; *Kikuchi*, 1983].

5. Conclusions

High-resolution electromagnetic wave data measured by the DEMETER spacecraft (2004–2010) during the periods of active Burst mode were used to investigate the influence of PLHR at frequencies corresponding to low harmonics of the base power system frequency (50/60 Hz, depending on the region). We have shown that the wave intensity at these frequencies is significantly enhanced above industrialized areas and that the frequencies at which the wave intensities are increased are in excellent agreement with the base power system frequencies just below the satellite location. No significant increase of the wave intensity is observed at geomagnetically conjugate regions, indicating that the PLHR effects are limited primarily to the hemisphere of origin.

We have investigated a possible presence of the weekend effect; i.e., we have verified whether the intensity increase related to PLHR follows a week cycle of the power consumption or not. Such an effect might be

possibly present in the European region, but it is very weak. PLHR effects are less often detected in the summer, which is likely due to the radiation being obscured by intense lightning-generated emissions and/or more attenuated when it crosses the ionosphere. This difference is smaller in the U.S. region than in the European region, in agreement with the respective monthly variations of the power consumption. The analysis of the frequency spectra observed by DEMETER reveals that the intensity increase related to PLHR is routinely observed not only at base power system frequencies but also at their low odd harmonics. No significant increase of the wave intensity at low even harmonics of the base power system frequencies was detected. Finally, we verified the relation of PLHR intensity to GICs, and we showed that the effect of PLHR is more pronounced at the times of high GIC proxy during the night.

Acknowledgments

DEMETER was a CNES mission. We thank the engineers from CNES and scientific laboratories (CBK, IRAP, LPC2E, LPP, SSD of ESTEC) who largely contributed to the success of this mission. DEMETER data are accessible from http://cdpp2.cnes.fr/cdpp. SuperMAG data are accessible from http://supermag.jhuapl.edu. Data used to calculate the average annual electric power consumption in 2004–2010 for individual countries are available from http://data.worldbank.org/indicator/EG.USE.ELEC.KH. Data used to calculate the U.S. electric power consumption as a function of day of week are available from http://www.ferc.gov/docs-filing/forms/form-714/data.asp. Data with the monthly variation of the electric power consumption in the European region are available from https://www.entsoe.eu/publications/statistics/monthly-statistics. Data with the monthly variation of the U.S. electric power consumption are available from http://www.eia.gov/electricity/monthly. HRMC LIS/OTD gridded climatology data set is available from http://lightning.nsstc.nasa.gov/data/data_lis-otd-climatology.html. This work was supported by GACR grants 15-01775Y and 14-31899S, MSMT grant LH 12231, and by the Praemium Academiae award from the CAS.

Michael Balikhin thanks two reviewers for their assistance in evaluating this paper.

References

Ando, Y., M. Hayakawa, and O. A. Molchanov (2002), Theoretical analysis on the penetration of power line harmonic radiation into the ionosphere, *Radio Sci.*, *37*(6), 1093, doi:10.1029/2001RS002486.

Berthelier, J. J., et al. (2006), ICE, the electric field experiment on DEMETER, *Planet. Space Sci.*, *54*, 456–471.

Bullough, K. (1995), Power line harmonic radiation: Sources and environmental effects, in *Handbook of Atmospheric Electrodynamics*, 2nd ed., vol. 2, edited by H. Volland, pp. 291–332, CRC Press, Boca Raton, Fla.

Cecil, D. J., D. E. Buechler, and R. J. Blakeslee (2014), Gridded lightning climatology from TRMM-LIS and OTD: Dataset description, *Atmos. Res.*, *135–136*, 404–414, doi:10.1016/j.atmosres.2012.06.028.

Chen, X., and Y. Zhang (2012), Detection and analysis of power system harmonics based on FPGA, in *Wireless Communications and Applications*, pp. 445–454, Volume 72 of the series Lecture Notes of the Institute for Computer Sciences, Social Informatics and Telecommunications Engineering, Springer, Berlin.

Forbes, K. F., and O. C. St. Cyr (2008), Solar activity and economic fundamentals: Evidence from 12 geographically disparate power grids, *Space Weather*, *6*, S10003, doi:10.1029/2007SW000350.

Forbes, K. F., and O. C. St. Cyr (2010), An anatomy of space weather's electricity market impact: Case of the PJM power grid and the performance of its 500 kV transformers, *Space Weather*, *8*, S09004, doi:10.1029/2009SW000498.

Fraser-Smith, A. C. (1979), A weekend increase in geomagnetic activity, *J. Geophys. Res.*, *84*, 2089–2096.

Gjerloev, J. W. (2012), The SuperMAG data processing technique, *J. Geophys. Res.*, *117*, A09213, doi:10.1029/2012JA017683.

Grady, W. M., and S. Santoso (2001), Understanding power system harmonics, *IEEE Power Eng. Rev.*, *21*(11), 8–11.

Hayashi, K., T. Oguti, T. Watanabe, K. Tsuruda, S. Kokobun, and R. E. Horita (1978), Power line harmonic enhancement during the sudden commencement of a magnetic storm, *Nature*, *275*, 627–529.

Jing, W., F. Jing-Jing, and Z. Chong (2014), Propagation characteristics of power line harmonic radiation in the ionosphere, *Chin. Phys. B*, *23*(3), 034102.

Karinen, A., K. Mursula, T. Ulich, and J. Manninen (2002), Does the magnetosphere behave differently on weekends?, *Ann. Geophys.*, *20*(8), 1137–1142.

Kikuchi, H. (1983), Overview of power-line harmonic radiation and its coupling to the ionosphere and magnetosphere, *Space Sci. Rev.*, *35*, 33–41.

Molchanov, O., and M. Parrot (1995), PLHR emissions observed on satellites, *J. Atmos. Terr. Phys.*, *57*(5), 493–505.

Molchanov, O. A., M. Parrot, M. M. Mogilevsky, and F. Lefeuvre (1991), A theory of PLHR emissions to explain the weekly variation of ELF data observed by a low-altitude satellite, *Ann. Geophys.*, *9*, 669–680.

Nunn, D., J. Manninen, T. Turunen, V. Trakhtengerts, and N. Erokhin (1999), On the nonlinear triggering of VLF emissions by power line harmonic radiation, *Ann. Geophys.*, *17*, 79–94.

Němec, F., O. Santolík, M. Parrot, and J. J. Berthelier (2006), Power line harmonic radiation (PLHR) observed by the DEMETER spacecraft, *J. Geophys. Res.*, *111*, A04308, doi:10.1029/2005JA011480.

Němec, F., O. Santolík, M. Parrot, and J. J. Berthelier (2007), Power line harmonic radiation: A systematic study using DEMETER spacecraft, *Adv. Space Res.*, *40*, 398–403.

Němec, F., O. Santolík, M. Parrot, and J. Bortnik (2008), Power line harmonic radiation observed by satellite: Properties and propagation through the ionosphere, *J. Geophys. Res.*, *113*, A08317, doi:10.1029/2008JA013184.

Němec, F., M. Parrot, and O. Santolík (2010), Influence of power line harmonic radiation on the VLF wave activity in the upper ionosphere: Is it capable to trigger new emissions?, *J. Geophys. Res.*, *115*, A11301, doi:10.1029/2010JA015718.

Park, C. G., and R. A. Helliwell (1983), Ground observations of power line radiation coupled to the ionosphere and magnetosphere, *Space Sci. Rev.*, *35*, 131–137.

Park, C. G., and T. R. Miller (1979), Sunday decreases in magnetospheric VLF wave activity, *J. Geophys. Res.*, *84*, 943–950.

Parrot, M. (1991), Daily variations of ELF data observed by a low-altitude satellite, *Geophys. Res. Lett.*, *18*(6), 1039–1042.

Parrot, M., and F. Němec (2009), MLR events and associated triggered emissions observed by DEMETER, *Adv. Space Res.*, *44*, 979–986.

Parrot, M., et al. (2006), The magnetic field experiment IMSC and its data processing onboard DEMETER: Scientific objectives, description and first results, *Planet. Space Sci.*, *54*, 441–455.

Parrot, M., F. Němec, and O. Santolík (2014), Statistical analysis of VLF radio emissions triggered by power line harmonic radiation and observed by the low-altitude satellite DEMETER, *J. Geophys. Res. Space Physics*, *119*, 5744–5754, doi:10.1002/2014JA020139.

Prakash, R., D. D. Gupta, and M. K. Singh (2009), Role of VLF power line harmonic radiation in precipitating energetic electrons at high latitude, *Indian J. Radio Space Phys.*, *38*, 74–79.

Rodger, C. J., N. R. Thomson, and R. L. Dowden (1995), VLF line radiation observed by satellite, *J. Geophys. Res.*, *100*(A4), 5681–5689.

Rodger, C. J., M. A. Clilverd, K. Yearby, and A. J. Smith (2000), Is magnetospheric line radiation man-made?, *J. Geophys. Res.*, *105*, 15,981–15,990.

Tatnall, A. R. L., J. P. Matthews, K. Bullough, and T. R. Kaiser (1983), Power-line harmonic radiation and the electron slot, *Space Sci. Rev.*, *35*, 139–173.

Tomizawa, I., and T. Yoshino (1985), Power line radiation observed by the satellite, *J. Geomagn. Geoelec.*, *37*, 309–327.
Viljanen, A., H. Nevanlinna, K. Pajunpää, and A. Pulkkinen (2001), Time derivative of the horizontal geomagnetic field as an activity indicator, *Ann. Geophys.*, *19*, 1107–1118.
Viljanen, A., E. I. Tanskanen, and A. Pulkkinen (2006), Relation between substorm characteristics and rapid temporal variations of the ground magnetic field, *Ann. Geophys.*, *24*, 725–733.